Article

*Discovery Medicine* 2025; 37(202): 2552–2566
https://doi.org/10.24976/Discov.Med.202537202.214

# $\alpha$-Syn-Induced mTOR Activation Impairs Autophagy and Mitophagy: Unraveling a Novel Mechanism in Parkinson's Disease Progression

Di An[1,†], Xiaoxi Liu[1,†], Ying Li[1], Yixian Li[1], Shasha Zhu[1,*]

[1]Neurology Department, The Affiliated Hospital of Hebei University, 071000 Baoding, Hebei, China
*Correspondence: an_dundun@163.com (Shasha Zhu)
[†]These authors contributed equally.
Submitted: 30 July 2025 Revised: 10 September 2025 Accepted: 24 September 2025 Published: 20 November 2025

**Background: Parkinson's disease (PD) is marked by dopaminergic neuron loss and motor deficits. Impaired autophagy and mitophagy contribute to PD, and $\alpha$-synuclein ($\alpha$-Syn) may worsen neurodegeneration by disrupting these pathways. This study investigates $\alpha$-Syn's role in aggravating motor deficits and dopaminergic neuron loss in 1-methyl-4-phenyl-1,2,3,6-tetrahydropyridine (MPTP)-induced PD mice, focusing on its inhibition of autophagy and mitophagy via mechanistic target of rapamycin (mTOR).**

**Methods: The MPTP-induced PD mouse model was used to study $\alpha$-Syn's role in PD. Motor function was assessed using the tail suspension, pole, and traction tests, while cognitive function was evaluated with the Morris water maze. $\alpha$-Syn and tyrosine hydroxylase (TH) levels in the substantia nigra were measured using Western blotting and immunohistochemistry. Autophagy and mitochondrial autophagy markers were analyzed via Western blotting. SH-SY5Y cells were treated with 1-methyl-4-phenylpyridinium ion ($MPP^+$) to model PD *in vitro*, followed by interventions $\alpha$-Syn and rapamycin (Rapa). Cell viability and apoptosis were assessed using 5-ethynyl-2′-deoxyuridine (EdU) and terminal deoxynucleotidyl transferase dUTP nick end labeling (TUNEL) staining, while autophagy and mitochondrial autophagy markers, reactive oxygen species (ROS) levels, and mitochondrial/lysosomal activity were analyzed using fluorescence staining and co-localization with MitoTracker and LysoTracker.**

**Results: The tail suspension, pole, and traction tests showed that MPTP treatment significantly impaired motor function, with $\alpha$-Syn further exacerbating deficits ($p < 0.05$). However, Rapa improved motor function. The Morris water maze test revealed increased escape latency and reduced swimming speed in the MPTP group, indicating spatial learning impairment, which worsened with $\alpha$-Syn but improved with $\alpha$-Syn+Rapa ($p < 0.05$). The spatial probe test showed decreased spatial memory in the MPTP + $\alpha$-Syn group, with significant improvement in the $\alpha$-Syn+Rapa group. Western blotting and immunohistochemistry showed that $\alpha$-Syn enhanced MPTP-induced dopaminergic neuron degeneration and inhibited autophagy and mitophagy ($p < 0.05$). *In vitro*, $\alpha$-Syn worsened SH-SY5Y cell viability and apoptosis, and inhibited autophagy and mitophagy by activating the mTOR pathway ($p < 0.05$).**

**Conclusions: $\alpha$-Syn induces dopaminergic neuron degeneration and worsens PD by inhibiting autophagy and mitophagy, but Rapa can partially reverse this by restoring these processes. Targeting autophagy and mitophagy may offer a promising strategy for PD treatment.**

**Keywords:** Parkinson's disease; $\alpha$-synuclein; autophagy; mitophagy; mTOR

## Introduction

Parkinson's disease (PD) is a chronic neurodegenerative disease primarily caused by a deficiency of dopamine, leading to motor impairments such as tremors, rigidity, and gait instability [1,2]. Cognitive impairment is a key symptom of PD, particularly in the later stages of the disease, where many patients experience a decline in cognitive function [3]. Cognitive impairment in PD is commonly referred to as Parkinson's disease dementia (PDD), and its incidence increases with disease progression [4]. Cognitive decline not only affects the patient's quality of life but also exacerbates their mental and social burden [5].

$\alpha$-synuclein ($\alpha$-Syn) is a 140-amino-acid presynaptic protein that plays a critical role in regulating synaptic vesicle trafficking and neurotransmitter release under physiological conditions [6]. However, under pathological circumstances, $\alpha$-Syn undergoes and abnormal aggregation into oligomers and fibrillar structures [7]. The abnormal accumulation of $\alpha$-Syn is believed to interfere with cellular processes, including autophagy and mitophagy, both of which are crucial for maintaining neuronal health [8,9].

The role of autophagy in PD has garnered widespread attention, as this cellular process is responsible for degrading damaged organelles, including mitochondria and misfolded proteins [10]. Dysregulation of autophagy can lead

to the accumulation of toxic proteins such as α-Syn, exacerbating neuronal death [11]. Additionally, mitochondrial dysfunction is a prominent feature of PD, and impaired mitochondrial function contributes to increased oxidative stress and accelerates neurodegeneration [12]. However, the interplay between α-Syn, autophagy, and mitochondrial dysfunction remains unclear.

Rapamycin (Rapa) is a key regulator of autophagy and cellular metabolism [13]. Under normal conditions, mechanistic target of rapamycin (mTOR) inhibits autophagy by suppressing critical autophagy-related proteins [14]. In PD, activation of mTOR signaling further inhibits autophagy, promoting the accumulation of α-Syn and impairing mitochondrial function [15]. Conversely, inhibition of mTOR using drugs like Rapa can enhance autophagic activity, reduce α-Syn aggregation, and alleviate mitochondrial damage [15]. Recent studies suggest that modulating the mTOR signaling pathway to promote autophagy offers a potential therapeutic strategy for PD [16,17].

The 1-methyl-4-phenyl-1,2,3,6-tetrahydropyridine (MPTP) model is a well-established and widely used experimental model in PD research [18]. This study seeks to examine the role of α-Syn in exacerbating motor deficits and dopaminergic neuronal degeneration in the MPTP-induced PD mouse model, with a focus on exploring the molecular mechanisms underlying autophagy, mitochondrial dysfunction, and the mTOR signaling pathway. Additionally, we examined the therapeutic potential of the autophagy inducer Rapa and investigated its effects on improving PD symptoms by enhancing autophagic activity and restoring mitochondrial function. In addition to deciphering the role of α-Syn in the progression of PD, this study also attempted to evaluate the potential of autophagy regulation as a therapeutic strategy for this debilitating disease.

## Materials and Methods

### *Establishment and Treatment of the PD Mouse Model*

Forty male C57BL/6J mice aged 8–12 weeks and weighing 20–25 g were acquired from Shanghai Model Organisms (Shanghai, China). The mice were randomly assigned into four groups using a random number table: Control group, MPTP-treated group, MPTP + α-Syn recombinant protein-treated group, and MPTP + α-Syn + Rapa-treated group. To establish a PD mouse model, injection of MPTP (HY-15608, MedChemExpress, Princeton, NJ, USA) into the animals was performed [19]. In the MPTP-treated group, mice received an intraperitoneal injection of MPTP solution (20 mg/kg) once daily for 7 consecutive days. In the MPTP + α-Syn group, α-Syn recombinant protein (ab316039, Abcam, Cambridge, UK) (1 mg/kg) was administered intraperitoneally in addition to MPTP treatment, once daily for 7 days. In the MPTP + α-Syn + Rapa group, both α-Syn recombinant protein (1 mg/kg) and Rapa (5 mg/kg) (S1039, Selleck, Houston, TX, USA) were injected intraperitoneally along with MPTP, once daily for 7 days. The control group was injected with physiological saline (25 mL/kg) intraperitoneally. The experiment duration was 14 days, and at the conclusion of the study, the mice were euthanized by intraperitoneal injection of 3% pentobarbital sodium (110 mg/kg) (P3761, Sigma-Aldrich, Darmstadt, Germany), and their brain tissues were harvested.

### *Tail Suspension Test*

In the tail suspension test, each mouse was suspended by its tail in a specialized testing apparatus, with the tail typically taped at the middle to ensure the body hangs vertically. The mouse usually struggles for a few seconds before entering a motionless state. The duration of struggling and remaining immobile during the suspension was recorded.

### *Pole Test*

A vertical wooden pole (approximately 50 cm in height and 1 cm in diameter) was used. The mouse was placed at the bottom of the pole, facing upward. The time taken for the mouse to climb to the top of the pole was recorded. In the event of falling, the time taken for the mouse to climb back up was recorded, or the observation continued until the end of the experiment. Each mouse underwent multiple trials (typically three), and the average climbing time was calculated.

### *Traction Test*

In the traction test, the mouse was positioned on a horizontal bar or a grid. The mouse's ability to grip the bar with both its forepaws and hindpaws was observed. The time taken for the mouse to hang on the bar before falling was measured. The duration for which the mouse can maintain its grip was recorded to assess grip strength and motor ability.

### *Morris Water Maze Test*

The experimental environment for conducting the Morris water maze test encompasses fixed visual cues (such as shapes or color markers) around the pool to help the mice with spatial navigation, and the lighting and visual cues are kept consistent throughout the experiment. The training phase lasts for 5 consecutive days, with 4 trials per day, where the starting positions were randomized, and each trial lasted a maximum of 60 seconds. After finding the platform, the mice must remain on it for 15 seconds to consolidate memory. If they fail to find the platform, the experimenter would guide them to it. On day 6, the platform was taken away for the probe trial. During this trial, the duration spent in the target quadrant and the frequency with which the mice cross the platform's original location are measured to evaluate spatial memory. Evaluation metrics include escape latency (time taken to find the platform), distance trav-

eled, swimming speed, platform crossing numbers, and the percentage of time spent in the target quadrant, all of which provide a comprehensive assessment of the mice's spatial learning and memory abilities.

### *Immunohistochemistry*

Mouse brain tissue was first fixed in 4% paraformaldehyde (P1110, Solarbio, Beijing, China), sectioned, dewaxed, and rehydrated. Antigen retrieval was performed using Tris-EDTA (C1038, pH 9.0, Solarbio, Beijing, China) at 100 °C for 20 minutes. The tissue was blocked with 5% normal serum for 30 minutes. The tyrosine hydroxylase (TH) antibody (1:500, sc-25269, Santa Cruz Biotechnology, Inc., Dallas, TX, USA) was incubated at room temperature for 1 hour, followed by three washes. The horseradish peroxidase (HRP)-conjugated secondary antibody (1:1000, ab6728, Abcam, Cambridge, UK) was incubated for 30 minutes, and the tissue was washed three times. 3,3′-diaminobenzidine (DAB) staining (DA1010, Solarbio, Beijing, China) was performed for visualization. After DAB staining, the reaction was terminated with distilled water, and the tissue was dehydrated and cleared. The sections were mounted using neutral resin mounting medium. TH expression was analyzed using an optical microscope (DMi8, Leica Microsystems, Wetzlar, Germany).

### *Hematoxylin and Eosin Staining*

Hematoxylin-eosin (HE) staining kit was purchased from Solarbio (G1120, Beijing, China). Brain tissue specimens procured from the experimental mice were fixed, dehydrated, cleared, and embedded in paraffin. The specimen paraffin blocks were then sectioned into 5 µm thick slices and placed on glass slides. The sections were deparaffinized and hydrated. The slides were stained with hematoxylin solution for 10 minutes, followed by washing, differentiation, and bluing. The sections were then stained with eosin solution for 10 minutes, washed, dehydrated, cleared, and mounted with neutral resin mounting medium. The slides were observed and analyzed under an optical microscope (BX53, Olympus, Tokyo, Japan).

### *Cell Culture*

SH-SY5Y cells were cultured in Dulbecco's Modified Eagle Medium/Nutrient Mixture F-12 (DMEM/F-12; 12400024, Gibco, Waltham, MA, USA) containing 10% fetal bovine serum (FBS) and supplemented with 100 U/mL penicillin and 100 µg/mL streptomycin to prevent contamination. The cells were maintained at 37 °C in a 5% $CO_2$ atmosphere. The cells were passaged upon reaching 80% confluence. The SH-SY5Y cells were authenticated by STR profiling and confirmed to be free of mycoplasma contamination.

### *Cell Treatment*

SH-SY5Y cells in the logarithmic growth phase were used in the experiment. The cells were randomly divided into four groups: Control group, 1-methyl-4-phenylpyridinium ion ($MPP^+$) (0.5 mM; ab144783, Abcam, Cambridge, UK) group, $MPP^+$ + $\alpha$-Syn recombinant protein (1 µM) group, and $MPP^+$ + $\alpha$-Syn + Rapa (1 µM) group. After 24 hours of treatment, cell viability was assessed. In the $MPP^+$ + $\alpha$-Syn recombinant protein (1 mM) group and the $MPP^+$ + $\alpha$-Syn + Rapa (5 µM) group, $\alpha$-Syn or $\alpha$-Syn + Rapa intervention was administered 3 hours after $MPP^+$ treatment.

### *Cell Counting Kit-8 (CCK-8) Assay*

Cells were seeded into a 96-well plate at 10,000 cells per well and cultured for 12 hours to allow for attachment. According to the experimental design, different treatments were added (reference cells), and the cells were cultured for 24 hours. Then, 10 µL of CCK-8 reagent (CA1210, Solarbio, Beijing, China) was added to each well, mixed, and incubated at 37 °C in a 5% $CO_2$ atmosphere for 12 hours. An additional 10 µL of CCK-8 reagent was added. Absorbance was measured at 450 nm using a microplate reader (BioTek Epoch 2, BioTek Instruments, Winooski, VT, USA).

### *Western Blotting*

Cells and tissues were lysed using lysis buffer (R0100, Solarbio, Beijing, China), followed by centrifugation (12,000 ×g, 4 °C for 15 minutes) to collect the protein supernatant. Protein concentration was quantified using the BCA assay (PC0020, Solarbio, Beijing, China). Proteins were denatured with sodium dodecyl sulfate (SDS) (S8010, Solarbio, Beijing, China) sample buffer and heated. Protein samples were loaded and subjected to electrophoresis across the stacking and separating gels. A wet transfer system was used to transfer proteins from the gel to a polyvinylidene fluoride (PVDF) membrane (YA1701, Solarbio, Beijing, China). The membrane was incubated overnight at 4 °C with primary antibodies targeting $\alpha$-Syn (1:1000, ab212184), TH (1:1000, ab137869), microtubule-associated protein 1 light chain 3 (LC3, 1:1000, ab192890), sequestosome 1 (p62, 1:1000, ab109012), PTEN-induced kinase 1 (PINK1, 1:1000, 23274-1-AP, Proteintech, Wuhan, China), cytochrome c oxidase subunit 4 (COX4, 1:1000, ab202554), phosphorylated cytochrome c oxidase subunit 4 (p-COX4, 1:1000, PA5-114563, Invitrogen, Carlsbad, CA, USA), phosphorylated AKT (p-AKT, 1:1000, ab38449), protein kinase B (AKT, 1:1000, ab8805), phosphorylated mechanistic target of rapamycin (p-mTOR, 1:1000, ab109268), mechanistic target of rapamycin (mTOR, 1:1000, ab134903), and glyceraldehyde-3-phosphate dehydrogenase (GAPDH) (1:1000, ab9485). The membrane was incubated with HRP-conjugated secondary antibody (1:1000, ab6721) for 1 hour at room temperature. After both primary and secondary

antibody incubations, the membrane was washed. Enhanced chemiluminescence (ECL) reagent (SW2010, Solarbio, Beijing, China) was added, and protein bands were observed using a chemiluminescence system (Gel Doc XR+, Bio-Rad Laboratories, Hercules, CA, USA). ImageJ software (version 1.5f, National Institutes of Health (NIH), Bethesda, MD, USA) was used for quantitative analysis of the images. Unless otherwise specified, all antibodies were purchased from Abcam (Cambridge, UK).

### *EdU Staining*

The cells were seeded in a culture plate and incubated until they achieved 60% confluence. 5-ethynyl-2′-deoxyuridine (EdU) solution was added to the culture plate and incubated for 6 hours. After incubation, the cells were fixed for 10 minutes. The cell membrane was then permeabilized for 5 minutes using 0.1% Triton X-100. The EdU staining was performed using the BeyoClick™ EdU-488 kit (C0071S, Beyotime, Shanghai, China) according to the manufacturer's instructions. 4′,6-diamidino-2-phenylindole (DAPI) dye was added subsequently for a 5-minute incubation to stain the nuclei. The EdU-positive cells were observed and photographed using a fluorescence microscope (DM6 B, Leica Microsystems, Wetzlar, Baden-Württemberg, Germany). ImageJ software (version 1.5f, NIH, Bethesda, MD, USA) was used for quantitative analysis of the images.

### *TUNEL Staining*

The cells were seeded in an appropriate culture plate. Following fixation and permeabilization, the One-step terminal deoxynucleotidyl transferase dUTP nick end labeling (TUNEL) Fluorescein Isothiocyanate Apoptosis Detection Kit (C1089, Beyotime, Shanghai, China) was utilized for TUNEL staining in accordance with the manufacturer's instructions. DAPI dye (C0065, Solarbio, Beijing, China) was added for a 5-minute incubation to stain the nuclei. A fluorescence microscope (DM6 B, Leica Microsystems, Wetzlar, Baden-Württemberg, Germany) was utilized to observe TUNEL-positive cells and capture their images. ImageJ software was used for quantitative analysis of the images.

### *ROS Staining*

The cells were seeded in a 6-well plate and cultured until reaching 80% confluence. An appropriate amount of DCFH-DA (10 μM; D6470, Solarbio, Beijing, China) was added to the passaged cells and incubated at 37 °C for 20 minutes, away from the light. The cells were then washed to remove excess probe. DAPI dye (C0065, Solarbio, Beijing, China) was added for a 5-minute incubation to stain the nuclei. A fluorescence microscope (DM6 B, Leica Microsystems, Wetzlar, Baden-Württemberg, Germany) was used to observe reactive oxygen species (ROS) fluorescence signals in the cells (excitation at 488 nm, emission at 525 nm). ImageJ software was used for quantitative analysis of the images.

### *MitoTracker and LysoTracker Co-localization Staining*

The cells were seeded in a 6-well plate and cultured until they achieved 70% confluence. MitoTracker dye (50 nM; M9940, Solarbio, Beijing, China) was added to the cell culture, which was then incubated in the dark at 37 °C for 30 minutes. Subsequently, the cells were washed to remove unbound dye. LysoTracker dye (50 nM; IF1850, Solarbio, Beijing, China) was added to the cell culture, which was then incubated in the dark at 37 °C for 30 minutes. Afterward, excess dye was removed through washing. The cells were fixed with a cell fixation solution for 10 minutes. The cell membrane was permeabilized for 5 minutes using 0.1% Triton X-100. The cells were blocked with 5% bovine serum albumin for 1 hour. DAPI dye (C0065, Solarbio, Beijing, China) was added for a 5-minute incubation to stain the nuclei. The cells were washed to remove unbound dye. A fluorescence microscope (DM6 B, Leica Microsystems, Wetzlar, Baden-Württemberg, Germany) was utilized to detect signals from different dye labels and capture co-localization images.

### *Statistical Analysis*

Data are presented as mean ± standard error of the mean. All statistical analyses were performed using GraphPad Prism 9.0 (GraphPad Software, San Diego, CA, USA). One-way analysis of variance (ANOVA) followed by Tukey's post hoc test was used for statistical comparisons between means. A $p < 0.05$ was considered statistically significant.

## Results

### *α-Syn Exacerbates Motor Deficits in MPTP-Induced PD Mice*

We evaluated the effects of α-Syn and Rapa on the motor abilities of MPTP-induced PD model mice using the tail suspension test, pole test, and traction test. The results of the tail suspension test (Fig. 1a) showed that a significant reduction in struggle time was observed in the MPTP group when compared with controls ($p < 0.001$). Additionally, the MPTP + α-Syn group had a much lower struggle time than the MPTP group. After the administration of Rapa, the struggle time was significantly increased ($p < 0.001$). The pole test results (Fig. 1b) revealed that mice in the MPTP group exhibited a markedly longer climbing time than those in the control group ($p < 0.001$). The MPTP + α-Syn group had a significantly longer climbing time than the MPTP group ($p < 0.001$). However, the climbing time of the MPTP + α-Syn + Rapa group was significantly shorter than that of the MPTP + α-Syn group ($p < 0.001$). The re-

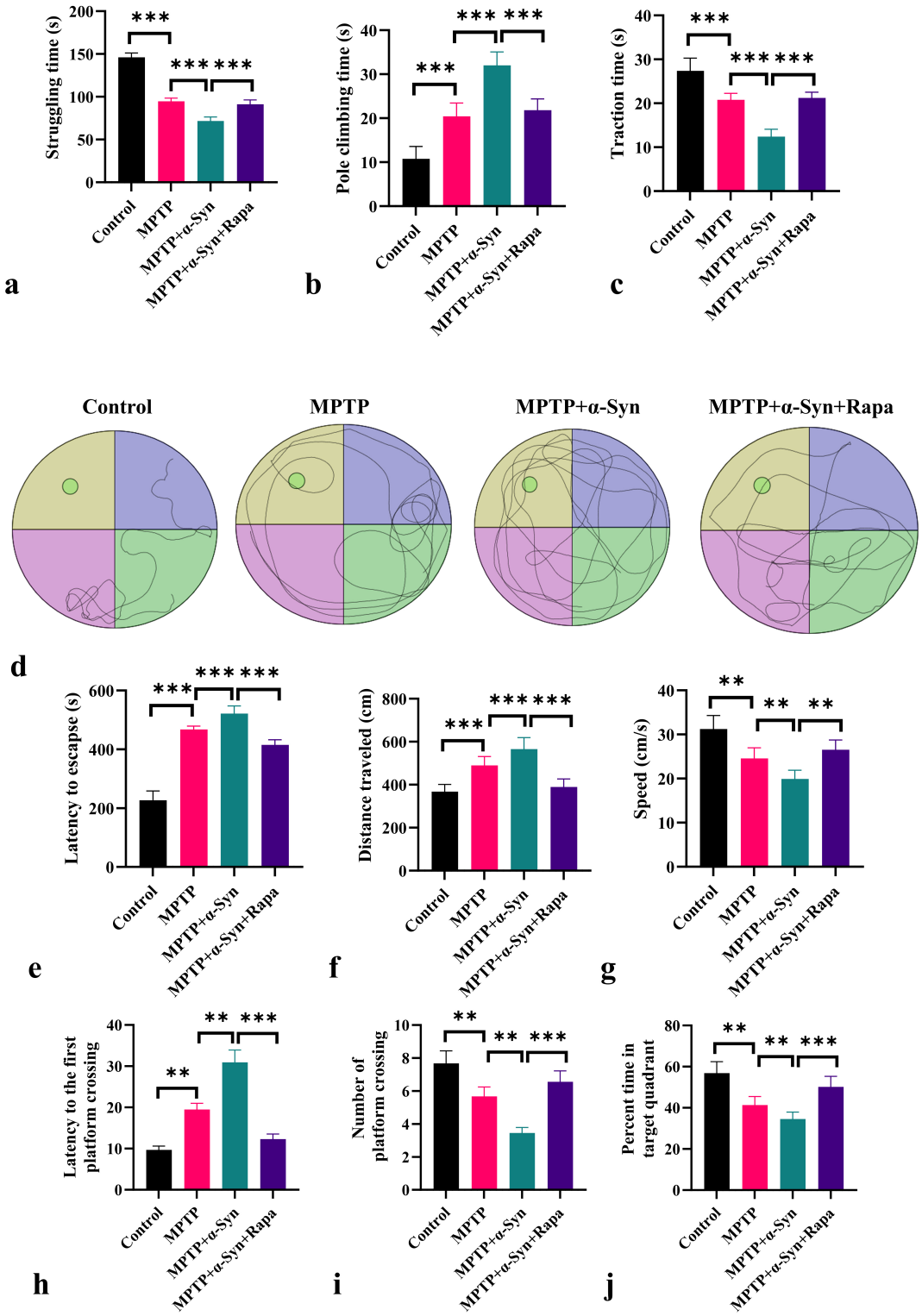


**Fig. 1. $\alpha$-Syn exacerbates motor deficits in MPTP-induced PD mice.** (a–c) Results of the tail suspension test (a), pole test (b), and traction test (c), which were used to assess the motor function of the mice. (d–j) In the Morris water maze test, the movement trajectory (d), escape latency (e), distance traveled (f), swimming speed (g), latency to the first platform crossing (h), number of platform crossings (i), and percentage of time spent in the target quadrant (j) were recorded for each group of mice. $n = 10$. $^{**}p < 0.01$, $^{***}p < 0.001$. Abbreviations: $\alpha$-Syn, $\alpha$-synuclein protein; MPTP, 1-methyl-4-phenyl-1,2,3,6-tetrahydropyridine; Rapa, rapamycin; PD, Parkinson's disease.

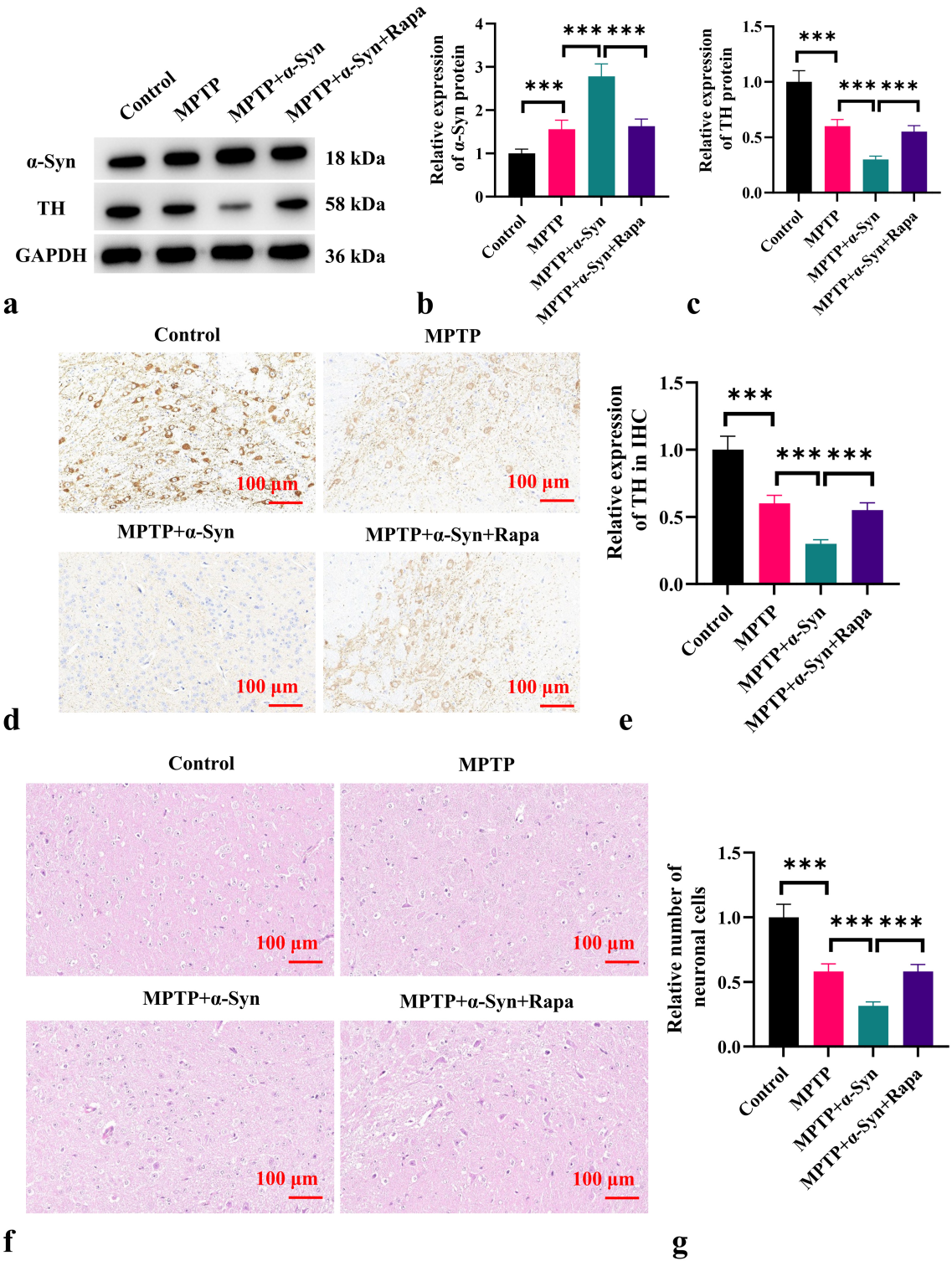


**Fig. 2. $\alpha$-Syn exacerbates dopaminergic neuron degeneration in MPTP-induced PD mice.** (a–c) Changes in TH and $\alpha$-Syn protein levels in mouse brain tissue after different treatments. (d,e) Immunohistochemical analysis of TH protein expression in mouse brain tissue. (f) Hematoxylin & eosin staining results of mouse brain tissue. (g) Relative number of neuronal cells. $n = 10$. ***$p < 0.001$. Abbreviations: TH, tyrosine hydroxylase; HE, hematoxylin and eosin; GAPDH, glyceraldehyde 3-phosphate dehydrogenase.

sults of the traction test (Fig. 1c) showed that the grip time of the MPTP group was notably lower than that of the control group ($p < 0.001$). A further significant decrease in grip time was observed in the MPTP + $\alpha$-Syn group relative to the MPTP group ($p < 0.001$). After the addition of Rapa, the grip time of the mice was significantly increased

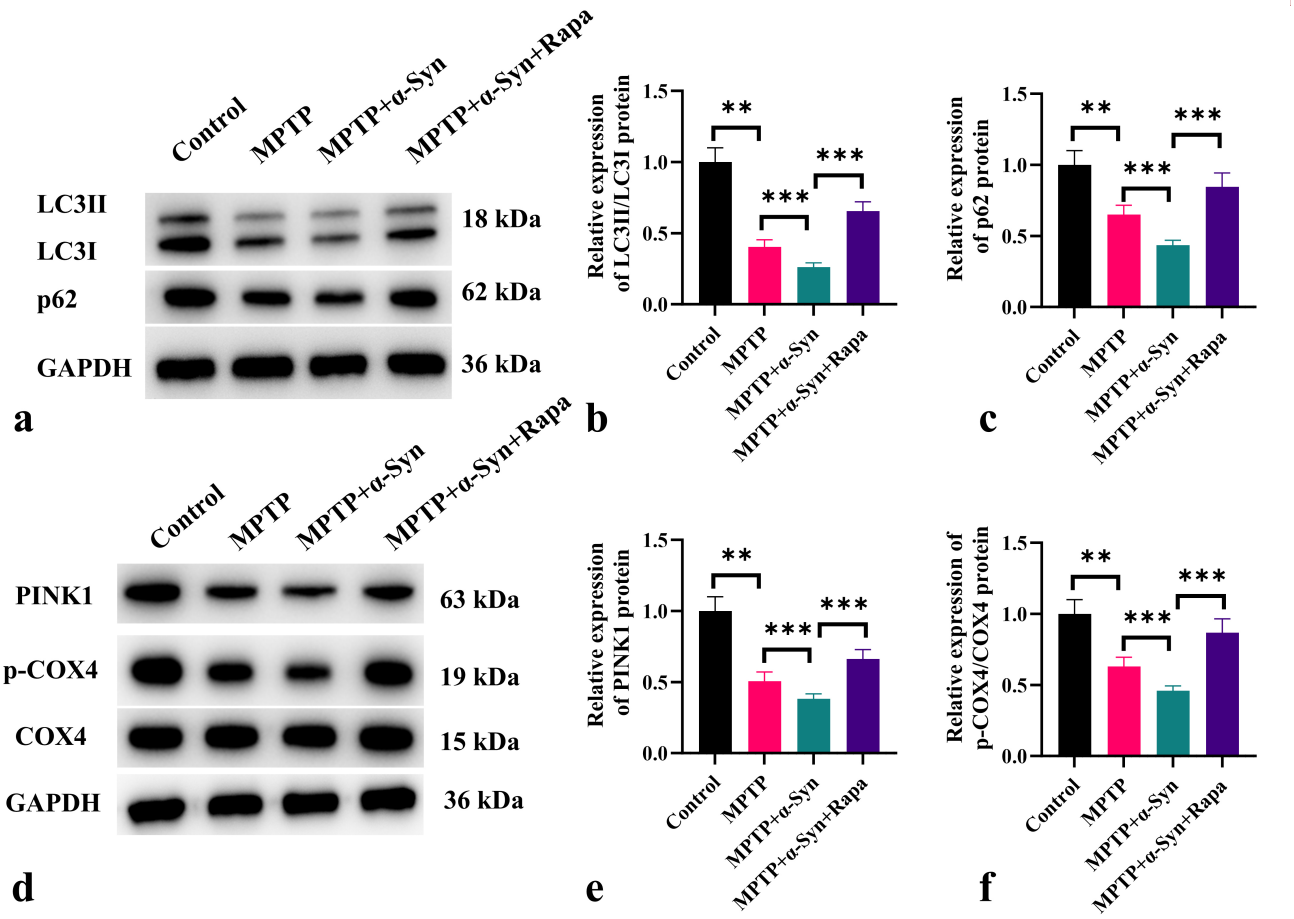


**Fig. 3. $\alpha$-Syn promotes the progression of PD by inhibiting autophagy and mitophagy.** (a–c) Changes in the levels of autophagy-related proteins LC3II/LC3I and p62 in mouse brain tissue after different treatments. (d–f) Changes in the levels of mitophagy-related proteins PINK1, p-COX4, and COX4 in mouse brain tissue after different treatments. $n = 10$. $^{**}p < 0.01$, $^{***}p < 0.001$. Abbreviations: COX4, cytochrome c oxidase subunit 4; p-COX4, phosphorylated COX4; LC3II/LC3I, microtubule-associated protein 1A/1B-light chain 3; p62, sequestosome 1; PINK1, PTEN-induced kinase 1.

compared to the MPTP + $\alpha$-Syn group ($p < 0.001$). In the Morris water maze test, compared to the control group, the MPTP group showed significantly increased escape latency and distance traveled by the mice ($p < 0.001$). Significant increases in escape latency and travel distance were also observed in the MPTP + $\alpha$-Syn group when compared with the MPTP group ($p < 0.001$) (Fig. 1d–f). In contrast, the escape latency and distance traveled in the MPTP + $\alpha$-Syn + Rapa group were significantly lower than in the MPTP + $\alpha$-Syn group ($p < 0.001$) (Fig. 1d–f). These results suggest that $\alpha$-Syn exacerbated the impairment of spatial learning in mice. Fig. 1g illustrates a marked reduction in swimming speed in the MPTP group relative to the control group ($p < 0.01$), along with a further significant decrease observed in the MPTP + $\alpha$-Syn group compared to the MPTP group ($p < 0.01$). Following the addition of Rapa, the swimming speed of the mice significantly increased compared to the MPTP + $\alpha$-Syn group ($p < 0.01$) (Fig. 1g). Subsequently, a spatial probe test was performed to assess the spatial memory of the mice (Fig. 1h–j). Compared to the MPTP group, the MPTP + $\alpha$-Syn group showed a significant increase in latency to the first platform crossing ($p < 0.01$), a reduction in the total number of platform crossings, and a decrease in the percentage of time spent in the target quadrant ($p < 0.01$), indicating impaired memory. In contrast, the MPTP + $\alpha$-Syn + Rapa group exhibited a significantly decreased latency to the first platform crossing ($p < 0.001$), alongside a notable rise in the number of platform crossings and the duration spent in the target quadrant compared to the MPTP + $\alpha$-Syn group ($p < 0.001$).

### *$\alpha$-Syn Exacerbates Dopamine Neuron Degeneration in MPTP-Induced PD Mice*

Western blot results indicate that $\alpha$-Syn protein expression was significantly greater in the MPTP group compared to the control group ($p < 0.001$). After the addition of $\alpha$-Syn recombinant protein, the $\alpha$-Syn protein level was even significantly elevated in the MPTP + $\alpha$-Syn group relative to the MPTP group ($p < 0.001$). Compared to the MPTP + $\alpha$-Syn group, the addition of Rapa resulted in a

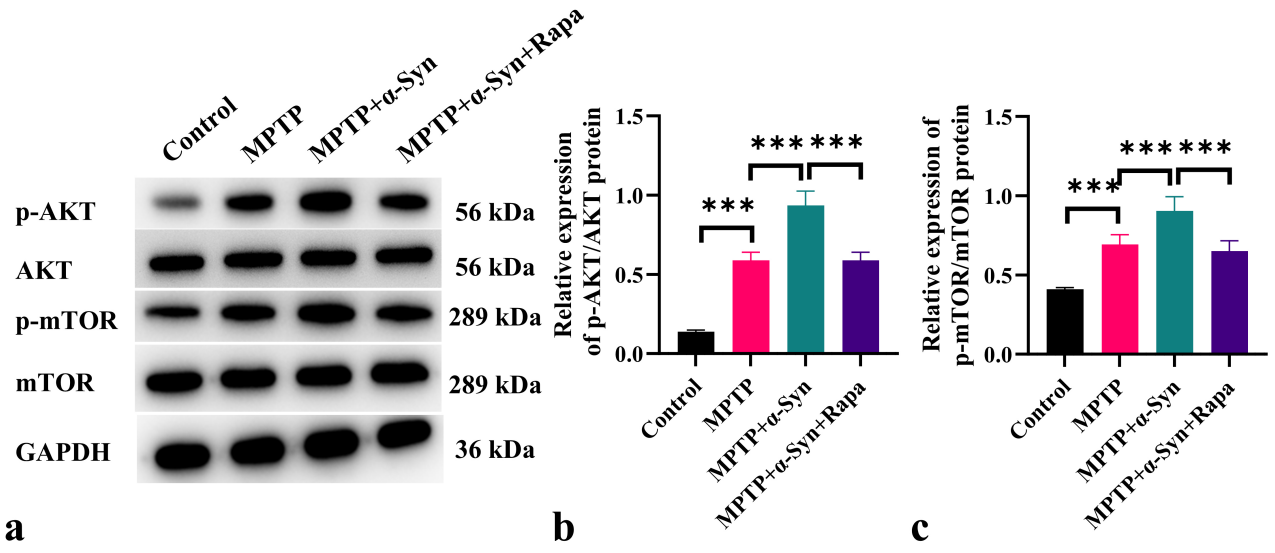


**Fig. 4. $\alpha$-Syn promotes the progression of PD by activating the mTOR signaling pathway, which inhibits autophagy and mitophagy.** (a) Western blot analysis of p-AKT, AKT, p-mTOR, and mTOR proteins across the treatment groups, and (b,c) quantitative analysis of the p-AKT/AKT and p-mTOR/mTOR proteins in mouse brain tissue after different treatments. $n = 10$. ***$p < 0.001$. Abbreviations: AKT, protein kinase B; p-AKT, phosphorylated AKT; mTOR, mechanistic target of rapamycin; p-mTOR, phosphorylated mTOR.

significant reduction in the $\alpha$-Syn protein level ($p < 0.001$) (Fig. 2a,b). Fig. 2a–c shows that the TH protein level in the MPTP group was markedly lower than that in the control group ($p < 0.001$), and the TH protein level in the MPTP + $\alpha$-Syn group was even lower than that in the MPTP group. Compared to the MPTP + $\alpha$-Syn group, Rapa administration significantly increased the TH protein level in the MPTP + $\alpha$-Syn + Rapa group ($p < 0.001$). An immunohistochemical approach was also utilized to detect the expression of TH in the brain tissue of the mice (Fig. 2d,e). The number of TH-positive neurons in the MPTP group was significantly lower than that in the control group, and the addition of $\alpha$-Syn recombinant protein further reduced the number of TH-positive neurons in the MPTP group. Compared to the MPTP + $\alpha$-Syn group, Rapa administration significantly increased the number of TH-positive neurons ($p < 0.001$). Additionally, HE staining was employed to analyze changes in brain tissue structure (Fig. 2f,g). In the control group, the neuronal cells were intact, well-formed, with round nuclei, clear boundaries, and evenly distributed chromatin. In the MPTP group, neuronal cells were significantly lost, accompanied by glial cell proliferation and inflammatory responses. The neurons showed shrinkage, nuclear condensation, and uneven chromatin. After $\alpha$-Syn recombinant protein treatment, the brain tissue damage and neuronal cell death in the MPTP group were further aggravated. Rapa treatment significantly improved the brain tissue damage and neuronal cell death induced by MPTP and $\alpha$-Syn.

### *$\alpha$-Syn Promotes PD Progression by Inhibiting Autophagy and Mitophagy*

Next, we measured the effects of $\alpha$-Syn and Rapa on autophagy and mitophagy in PD mice by means of Western blotting. The results in Fig. 3a–c show that after MPTP treatment, the expression of LC3II/LC3I and p62 was significantly reduced compared to the control group ($p < 0.01$). After the addition of $\alpha$-Syn, the decrease in LC3II/LC3I and p62 expression was even more pronounced compared to the MPTP group ($p < 0.001$). However, following the addition of Rapa, the expression of LC3II/LC3I and p62 was significantly elevated in the MPTP + $\alpha$-Syn + Rapa group compared to the MPTP + $\alpha$-Syn group ($p < 0.001$). PINK1 is an important regulatory protein involved in mitophagy, participating in the clearance of damaged mitochondria [20]. COX4 is a subunit of the mitochondrial respiratory chain complex, reflecting mitochondrial function. The phosphorylation status of p-COX4 may reflect its activity regulation [21]. The results in Fig. 3d–f show that in the MPTP group, the expression of PINK1 and p-COX4/COX4 was significantly reduced compared to the control group ($p < 0.01$). After the addition of $\alpha$-Syn, the expression of PINK1 and p-COX4/COX4 decreased even more significantly compared to the MPTP group ($p < 0.001$). After the addition of Rapa, the levels of PINK1 and p-COX4/COX4 were significantly increased in the MPTP + $\alpha$-Syn + Rapa group compared to the MPTP + $\alpha$-Syn group ($p < 0.001$).

### *α-Syn Promotes PD via mTOR Signaling Pathway-Mediated Autophagy and Mitophagy Inhibition*

The results in Fig. 4a–c show that in the MPTP group, MPTP treatment significantly increased the relative expression of p-AKT/AKT and p-mTOR/mTOR compared to the control group. The addition of α-Syn further enhanced the expression levels of p-AKT/AKT and p-mTOR/mTOR in the MPTP + α-Syn group relative to the MPTP group. Compared to the MPTP + α-Syn group, the expression of p-AKT/AKT and p-mTOR/mTOR in the MPTP + α-Syn + Rapa group was significantly decreased ($p < 0.001$).

### *α-Syn Suppresses Viability of $MPP^+$-Induced SH-SY5Y Cells*

EdU fluorescence staining results show (Fig. 5a,b) that compared to the control group, the $MPP^+$ group exhibited a significant reduction in the percentage of EdU-positive cells following 0.5 mM $MPP^+$ treatment ($p < 0.001$). Such a decrease was further exacerbated when $MPP^+$ was administered in combination with α-Syn (1 mM), marked by a more significant reduction in the percentage of EdU-positive cells compared to the $MPP^+$ group ($p < 0.001$). In the $MPP^+$ + α-Syn + Rapa group, the addition of 5 μM Rapa significantly increased the proportion of EdU-positive cells compared to the $MPP^+$ + α-Syn group ($p < 0.001$).

Fig. 5c,d shows that $MPP^+$ treatment significantly increased the proportion of apoptotic cells, with a notable increase in TUNEL-positive cells compared to the control group ($p < 0.001$). In the $MPP^+$ + α-Syn group, the proportion of apoptotic cells further increased following α-Syn treatment, as compared to the $MPP^+$ group ($p < 0.001$). In the $MPP^+$ + α-Syn + Rapa group, the addition of Rapa significantly reduced the proportion of TUNEL-positive cells, as compared to the $MPP^+$ + α-Syn group ($p < 0.001$).

Additionally, assessment of ROS levels in SH-SY5Y cells by means of fluorescence staining was conducted. The results in Fig. 5e,f show that when compared to the control group, the $MPP^+$ group exhibited a significant increase in ROS fluorescence intensity ($p < 0.001$). In the $MPP^+$ + α-Syn group, the ROS fluorescence intensity was further enhanced after α-Syn treatment, as compared to the $MPP^+$ group ($p < 0.001$). Our results also showed that the addition of Rapa significantly decreased the ROS fluorescence intensity in the $MPP^+$ + α-Syn + Rapa group compared to the $MPP^+$ + α-Syn group ($p < 0.001$).

### *α-Syn Promotes PD Progression by Inhibiting Autophagy and Mitophagy in SH-SY5Y Cells*

Next, we assessed the effects of α-Syn and Rapa on autophagy and mitophagy in SH-SY5Y cells through Western blotting. The results in Fig. 6a–c show that compared to the control group, the $MPP^+$ group displayed significantly decreased expression of LC3II/LC3I and p62 ($p < 0.001$). The addition of α-Syn further reduced the expression of LC3II/LC3I and p62 in the $MPP^+$ + α-Syn group compared to the $MPP^+$ group ($p < 0.001$). In the $MPP^+$ + α-Syn + Rapa group, the expression of LC3II/LC3I and p62 was restored, as compared to the $MPP^+$ + α-Syn group ($p < 0.001$). Fig. 6d–f shows that compared to the control group, the $MPP^+$ treatment group exhibited significantly lower expression of PINK1 and p-COX4/COX4. The expression of PINK1 and p-COX4/COX4 was further reduced in the $MPP^+$ + α-Syn group relative to the $MPP^+$ group ($p < 0.001$). However, the levels of PINK1 and p-COX4/COX4 significantly increased in the $MPP^+$ + α-Syn + Rapa group compared to the $MPP^+$ + α-Syn group ($p < 0.001$).

Additionally, we measured the fluorescence intensity and colocalization of MitoTracker and LysoTracker in SH-SY5Y cells by using immunofluorescence. The results in Fig. 6g show that compared to the control group, the $MPP^+$ group demonstrated significantly lower fluorescence intensity of Mito Tracker and Lyso Tracker, as well as a lower degree of colocalization. This suggests a reduction in autolysosomes. The $MPP^+$ + α-Syn co-treatment resulted in further decrease of the fluorescence intensity of MitoTracker and LysoTracker, further decimating autolysosomes. In contrast, in comparison to the $MPP^+$ + α-Syn group, the $MPP^+$ + α-Syn + Rapa group displayed enhanced fluorescence intensity of MitoTracker and LysoTracker, as well as an increased number of autolysosomes.

### *α-Syn Promotes PD Progression by Inhibiting SH-SY5Y Cell Autophagy and Mitophagy by Activating mTOR Signaling Pathway*

The results in Fig. 7a–c show that in the $MPP^+$ group, the relative expression of p-AKT/AKT and p-mTOR/mTOR was significantly increased compared to that observed in the control group. The expression levels of p-AKT/AKT and p-mTOR/mTOR were further enhanced in the $MPP^+$ + α-Syn group compared to the $MPP^+$ group. However, the $MPP^+$ + α-Syn + Rapa group exhibited significantly reduced expression of p-AKT/AKT and p-mTOR/mTOR compared to the $MPP^+$ + α-Syn group ($p < 0.001$).

## Discussion

The pathophysiology of PD is complex and involves oxidative stress, mitochondrial dysfunction, neuroinflammation, and impaired protein degradation pathways [22, 23]. This study aims to investigate the role of α-Syn in exacerbating motor deficits and dopaminergic neuronal degeneration in the MPTP-induced PD mouse model and explore the underlying molecular mechanisms, with a particular focus on autophagy, mitochondrial function, and the mTOR signaling pathway. Our findings indicate that α-Syn plays a critical role in amplifying MPTP-induced PD pathology, and autophagy regulation, especially through Rapa, holds potential therapeutic benefits.

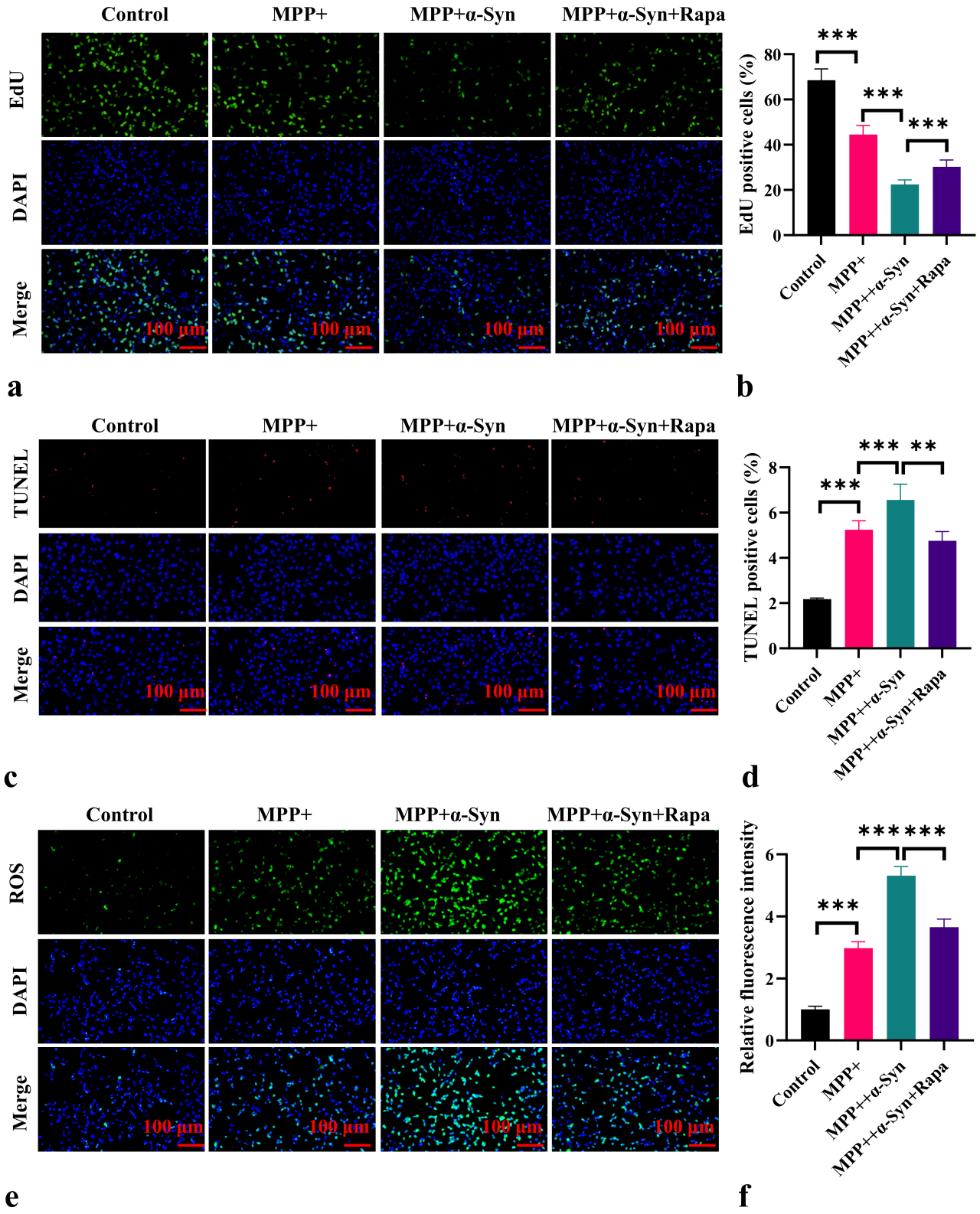


**Fig. 5. $\alpha$-Syn further decreases the viability of MPP$^+$-induced SH-SY5Y cells.** (a,b) EdU staining results showing the effects of different treatments on cell viability. (c,d) TUNEL staining results showing the effects of different treatments on cell apoptosis. (e,f) Fluorescence staining of ROS in the cells. $n = 6$. $^{**}p < 0.01$, $^{***}p < 0.001$. Abbreviations: DAPI, 4′,6-diamidino-2-phenylindole; EdU, 5-ethynyl-2′-deoxyuridine; MPP$^+$, 1-Methyl-4-phenylpyridinium; ROS, reactive oxygen species; TUNEL, terminal deoxynucleotidyl transferase dUTP nick-end labeling.

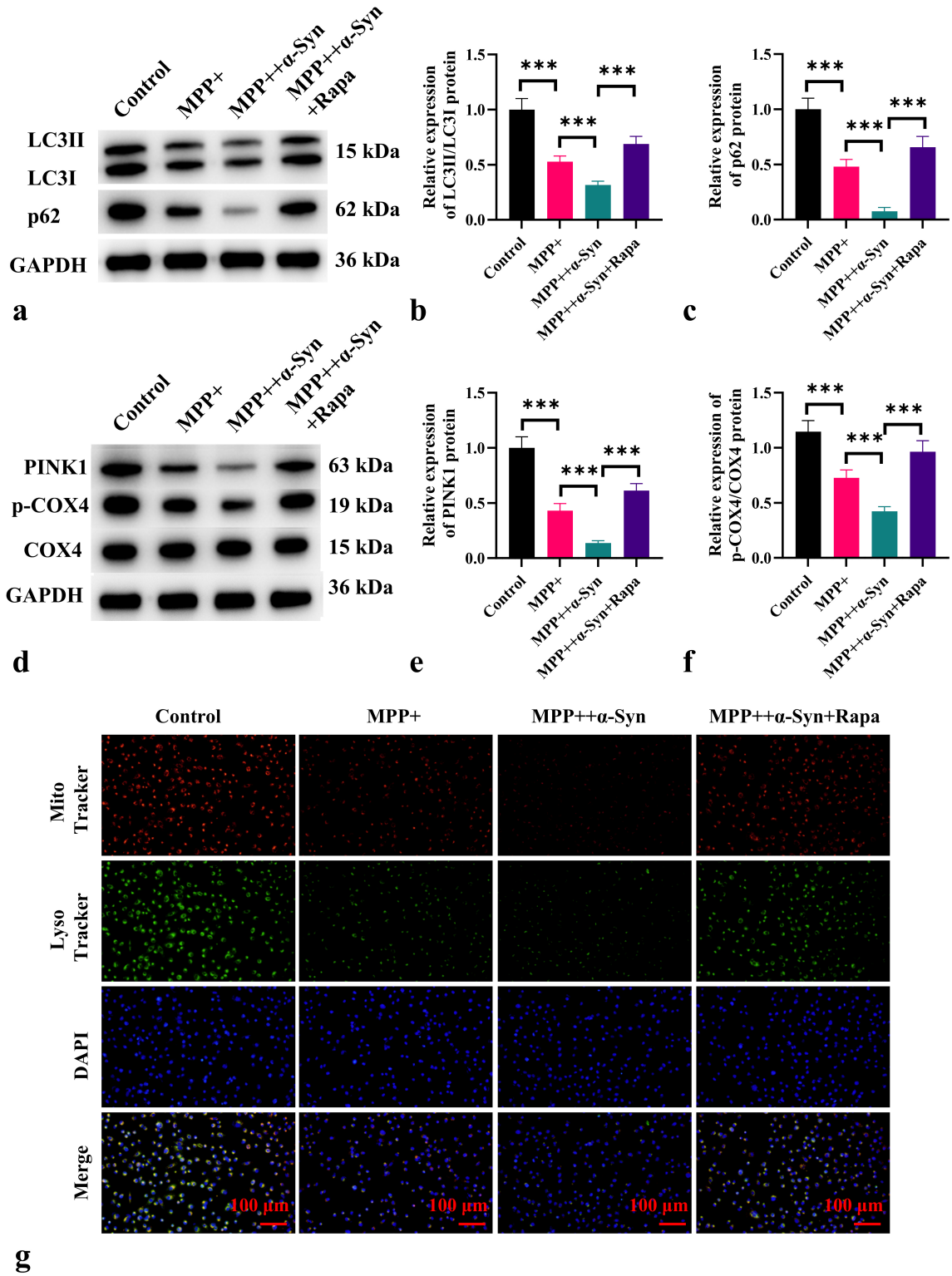


**Fig. 6. $\alpha$-Syn promotes the progression of PD by inhibiting autophagy and mitophagy in SH-SY5Y cells.** (a–c) Changes in the levels of autophagy-related proteins LC3II/LC3I and p62 after different treatments. (d–f) Changes in the levels of mitophagy-related proteins PINK1, p-COX4, and COX4 after different treatments. (g) Fluorescence staining images demonstrating the fluorescence intensity and colocalization of MitoTracker and LysoTracker in cells. $n = 10$. ***$p < 0.001$. Abbreviations: Lyso Tracker, LysoTracker lysosomal stain; MitoTracker, MitoTracker mitochondrial stain.

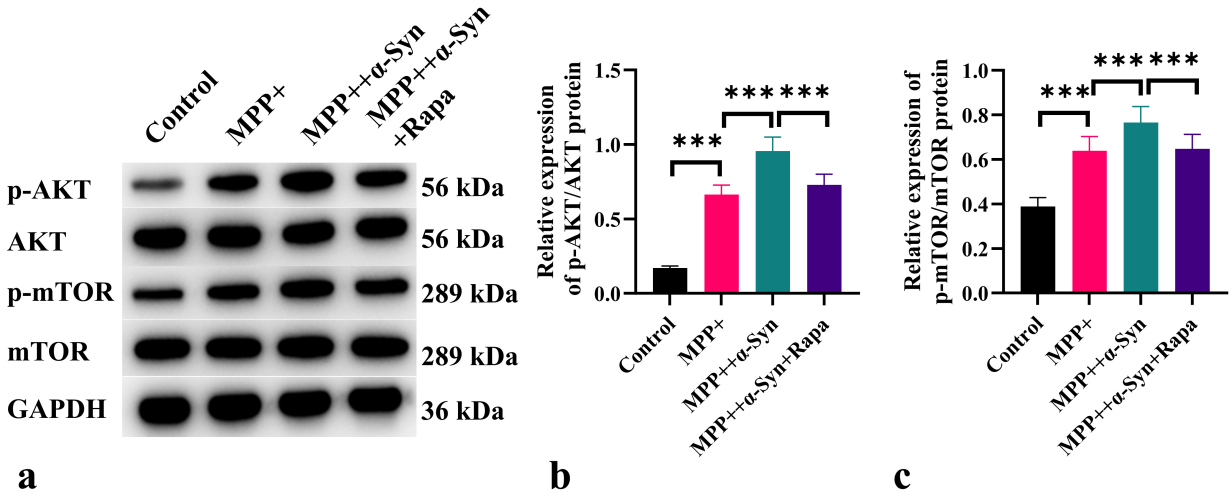


**Fig. 7. $\alpha$-Syn promotes the progression of PD by inhibiting SH-SY5Y cell autophagy and mitophagy through activation of the mTOR signaling pathway.** (a) Western blot analysis of the p-AKT, AKT, p-mTOR, and mTOR proteins across the treatment groups, and (b,c) quantitative analysis of the p-AKT/AKT and p-mTOR/mTOR proteins after different treatments. $n = 10$. ***$p < 0.001$.

This study demonstrates that the motor deficits induced by MPTP treatment are closely associated with the degeneration of dopaminergic neurons, consistent with pathological mechanisms of PD [24]. Motor dysfunction is a core clinical manifestation of PD, primarily caused by the loss of dopaminergic neurons in the substantia nigra. We observed significant motor impairments in the MPTP-treated mice, likely due to the loss of dopaminergic neuron function in the nigrostriatal pathway [25]. MPTP-induced PD mice exhibited significant motor deficits, which were further exacerbated by $\alpha$-Syn. However, Rapa partially reversed these impairments by restoring autophagy and mitophagy activity, thereby improving motor function. In addition, $\alpha$-Syn worsened spatial learning and memory deficits in the mice, while Rapa significantly restored these cognitive functions. Mechanistic analysis indicated that $\alpha$-Syn disrupted normal autophagy and mitophagy processes, leading to neuronal degeneration, whereas Rapa alleviated this damage by activating the autophagy pathway. The aggregation of $\alpha$-Syn may accelerate dopaminergic neuronal degeneration through direct toxicity or by exacerbating oxidative stress and neuroinflammation, leading to further deterioration of motor function [26,27]. Interestingly, the use of Rapa, an autophagy inducer, significantly improved the motor performance of mice in the MPTP + $\alpha$-Syn treatment group. This aligns with existing research indicating that enhancing autophagy can alleviate motor deficits in PD models [28]. We observed an improvement in motor function following Rapa treatment, which may be attributed to its ability to restore autophagic flux and clear damaged proteins, such as $\alpha$-Syn aggregates, thereby reducing neurotoxicity and promoting neuronal survival. These findings highlight the potential therapeutic role of autophagy enhancers in alleviating PD-related motor deficits.

The degeneration of dopaminergic neurons is a hallmark of PD and the primary cause of motor dysfunction [29]. This study demonstrates that MPTP treatment significantly reduced the expression of TH, a key marker protein of dopaminergic neurons. This reduction in TH levels is a recognized hallmark of dopaminergic neuronal degeneration in PD models. The addition of $\alpha$-Syn further exacerbated the decline in TH expression, indicating that $\alpha$-Syn plays a critical role in promoting the loss of dopaminergic neurons. Previous research has shown that $\alpha$-Syn aggregates directly impair dopaminergic neuronal function and accelerate their degeneration [30]. Furthermore, $\alpha$-Syn may enhance neuroinflammation and oxidative stress, further accelerating neuronal death. In this investigation, administration of Rapa significantly increased TH expression in the mice treated with MPTP and $\alpha$-Syn, providing mechanistic evidence for a previous study suggesting that activation of autophagy can reduce dopaminergic neuronal loss in PD models [31]. This finding implies that autophagy may exert protective effects by clearing $\alpha$-Syn aggregates, alleviating oxidative stress, and reducing inflammation, thereby preserving the function and survival of dopaminergic neurons. Thus, regulating autophagy, particularly through Rapa, could be an effective strategy to mitigate dopaminergic neuronal degeneration in PD.

Autophagy is a cellular process responsible for the degradation and recycling of damaged proteins and organelles, including misfolded proteins and dysfunctional mitochondria [32]. In PD, impaired autophagic flux leads to the accumulation of toxic proteins, such as $\alpha$-Syn, resulting in neuronal damage and disease progression. Our results show that MPTP treatment reduced the expression of key autophagy markers, LC3II/LC3I and p62, consistent with the previous study indicating autophagic dysfunction in PD

models [33]. We further found that α-Syn exacerbates this autophagic dysfunction, as evidenced by a more significant decrease in LC3II/LC3I and p62 levels in the MPTP + α-Syn group. This finding supports the hypothesis that α-Syn aggregates inhibit autophagic flux, leading to the accumulation of toxic proteins, thereby exacerbating neuronal damage. These results are consistent with previous research, which indicates that α-Syn aggregates directly hinder the autophagic degradation of misfolded proteins, thereby promoting neurodegeneration [33]. It is noteworthy that treatment with Rapa, an autophagy inducer, significantly reversed these autophagic defects. In the MPTP + α-Syn + Rapa group, the LC3II/LC3I levels increased, while the p62 levels decreased. This suggests that enhanced autophagy can restore the capacity of α-Syn aggregate clearance and alleviate associated neurotoxicity. This finding is consistent with other research that indicates autophagy activation can promote the degradation of α-Syn, thereby reducing its toxic effects in PD [34].

Mitochondrial dysfunction is a core feature of PD, as impaired mitochondrial quality control leads to the accumulation of damaged mitochondria, contributing to oxidative stress and neuronal death. In this study, we observed that MPTP treatment reduced the expression of PINK1 and COX4, both of which are key proteins in maintaining mitochondrial health and function. PINK1 is a mitochondrial kinase that plays an essential role in the clearance of damaged mitochondria through mitophagy. COX4 is a subunit of mitochondrial respiratory complex IV, reflecting mitochondrial function. We found that α-Syn further decreased the expression of PINK1 and COX4, suggesting that α-Syn exacerbates mitochondrial dysfunction and inhibits mitophagy. The addition of Rapa significantly increased the expression of PINK1 and COX4 in the MPTP + α-Syn + Rapa group, suggesting that enhanced autophagy can restore mitochondrial function and mitophagy. This is consistent with previous studies that highlight the crucial role of autophagy in maintaining mitochondrial quality control and preventing neurodegenerative diseases [35,36]. By promoting mitophagy, Rapa may facilitate the clearance of damaged mitochondria, reduce oxidative stress, and protect neurons from damage [37].

The mTOR signaling pathway is a key regulator of autophagy and cellular metabolism. In our study, we found that MPTP treatment increased the phosphorylation of AKT and mTOR, which is indicative of the mTOR pathway activation. α-Syn further enhanced this activation, suggesting that α-Syn may inhibit autophagy through the mTOR signaling pathway. Existing studies have shown that α-Syn is more likely to activate the mTOR pathway through indirect mechanisms rather than direct interaction. For example, some reports suggest that α-Syn can induce ROS accumulation and mitochondrial dysfunction, which subsequently activate the PI3K/AKT pathway, leading to mTOR activation [38]. In our *in vitro* experiments, we observed increased ROS levels and decreased mitochondrial membrane potential in the $MPP^+$ + α-Syn group, providing validation to the proposed mechanism. Additionally, it has been demonstrated that α-Syn may regulate the TSC1/2 complex, thereby indirectly relieving the inhibition on mTORC1 [39]. Our research findings are consistent with previous research, indicating that mTOR inhibition can promote autophagy and protect against neurodegeneration in PD models [40].

The MPTP model, while widely used in PD research, has several limitations: MPTP induces PD-like symptoms in mice and primates, but its effects do not fully replicate the complex pathophysiology of PD in humans. For instance, MPTP primarily targets dopaminergic neurons, whereas human PD involves a broader range of neurodegenerative processes. MPTP causes acute toxicity and rapid degeneration of dopaminergic neurons, whereas PD in humans typically develops gradually over years. Therefore, the unique attributes of the MPTP model in the disease development make it challenging to study the chronic aspects of PD progression. In addition, Lewy bodies—a hallmark of PD—do not form in the MPTP model. This limits the model's ability to replicate all aspects of PD pathology. MPTP-induced motor deficits in animals primarily reflect motor dysfunction but do not fully encompass the cognitive and psychiatric symptoms often observed in human PD patients. While non-human primates show symptoms similar to human PD, the MPTP model in rodents does not fully replicate the human disease. Rodents, for example, exhibit less severe motor deficits and may not develop the same cognitive impairments seen in humans. MPTP treatment typically causes acute damage, and long-term studies are often limited in scope. The model does not naturally encapsulate the long-term effects of PD that evolve over decades in humans.

In addition to animal experiments, we also used the SH-SY5Y neuroblastoma cell line in the present study to further investigate the role of α-Syn and Rapa in PD pathology. Similar to the animal studies, we found that α-Syn exacerbated $MPP^+$-induced inhibition of cell proliferation, apoptosis, and ROS generation. These results are consistent with previous research, suggesting that α-Syn aggregates induce cell apoptosis through oxidative stress [41]. Moreover, Rapa treatment reversed these effects, improving cell survival and attenuating oxidative stress. This suggests that autophagy enhancers may exert neuroprotective effects by alleviating oxidative stress, promoting the clearance of damaged proteins, and inhibiting neuronal apoptosis.

## Conclusions

This study suggests that α-Syn plays a crucial role in exacerbating MPTP-induced PD pathology, particularly in worsening motor deficits and dopaminergic neuronal degeneration. α-Syn exacerbates the pathological progression of PD by inhibiting autophagy and promoting mito-

chondrial dysfunction. The use of autophagy inducers such as Rapa can reverse these effects, improve motor function, reduce neuronal loss, and restore mitochondrial function. Therefore, autophagy inducers such as Rapa offer a potential therapeutic strategy to alleviate PD symptoms and delay disease progression.

## Availability of Data and Materials

The data that support the findings of this study are available from the corresponding author upon reasonable request.

## Author Contributions

DA and XXL designed the research study. YL, YXL and SSZ performed the research. DA, XXL and SSZ analyzed the data. All authors were involved in drafting the manuscript or revising it critically for important intellectual content. All authors read and approved the final manuscript. All authors have participated sufficiently in the work and agreed to be accountable for all aspects of the work.

## Ethics Approval and Consent to Participate

All animal experiments were approved by the Animal Ethical and Welfare Committee of Hebei University (Approval no. IACUC-2024009SR) and were performed in accordance with the Guidelines for the Care and Use of Laboratory Animals of Hebei University.

## Acknowledgment

Not applicable.

## Funding

This research was supported by Medical Science Research Project of Hebei, Grant No. 20260728, and Baoding Municipal Science and Technology Plan Project, Grant No. 2441ZF100.

## Conflict of Interest

The authors declare no conflict of interest.

## References

[1] Tolosa E, Garrido A, Scholz SW, Poewe W. Challenges in the diagnosis of Parkinson's disease. The Lancet. Neurology. 2021; 20: 385–397. https://doi.org/10.1016/S1474-4422(21)00030-2.

[2] Cattaneo C, Jost WH. Pain in Parkinson's Disease: Pathophysiology, Classification and Treatment. Journal of Integrative Neuroscience. 2023; 22: 132. https://doi.org/10.31083/j.jin2205132.

[3] Weintraub D, Aarsland D, Chaudhuri KR, Dobkin RD, Leentjens AF, Rodriguez-Violante M, *et al*. The neuropsychiatry of Parkinson's disease: advances and challenges. The Lancet. Neurology. 2022; 21: 89–102. https://doi.org/10.1016/S1474-4422(21)00330-6.

[4] Orgeta V, McDonald KR, Poliakoff E, Hindle JV, Clare L, Leroi I. Cognitive training interventions for dementia and mild cognitive impairment in Parkinson's disease. The Cochrane Database of Systematic Reviews. 2020; 2: CD011961. https://doi.org/10.1002/14651858.CD011961.pub2.

[5] Ye H, Robak LA, Yu M, Cykowski M, Shulman JM. Genetics and Pathogenesis of Parkinson's Syndrome. Annual Review of Pathology. 2023; 18: 95–121. https://doi.org/10.1146/annurev-pathmechdis-031521-034145.

[6] Lee J, Sung KW, Bae EJ, Yoon D, Kim D, Lee JS, *et al*. Targeted degradation of $\alpha$-synuclein aggregates in Parkinson's disease using the AUTOTAC technology. Molecular Neurodegeneration. 2023; 18: 41. https://doi.org/10.1186/s13024-023-00630-7.

[7] Mehra S, Sahay S, Maji SK. $\alpha$-Synuclein misfolding and aggregation: Implications in Parkinson's disease pathogenesis. Biochimica et Biophysica Acta. Proteins and Proteomics. 2019; 1867: 890–908. https://doi.org/10.1016/j.bbapap.2019.03.001.

[8] Prasertsuksri P, Kraokaew P, Pranweerapaiboon K, Sobhon P, Chaithirayanon K. Neuroprotection of Andrographolide against Neurotoxin $MPP^+$-Induced Apoptosis in SH-SY5Y Cells via Activating Mitophagy, Autophagy, and Antioxidant Activities. International Journal of Molecular Sciences. 2023; 24: 8528. https://doi.org/10.3390/ijms24108528.

[9] Basellini MJ, Kothuis JM, Comincini A, Pezzoli G, Cappelletti G, Mazzetti S. Pathological Pathways and Alpha-Synuclein in Parkinson's Disease: A View from the Periphery. Frontiers in Bioscience (Landmark Edition). 2023; 28: 33. https://doi.org/10.31083/j.fbl2802033.

[10] Lizama BN, Chu CT. Neuronal autophagy and mitophagy in Parkinson's disease. Molecular Aspects of Medicine. 2021; 82: 100972. https://doi.org/10.1016/j.mam.2021.100972.

[11] Tang Q, Gao P, Arzberger T, Höllerhage M, Herms J, Höglinger G, *et al*. Alpha-Synuclein defects autophagy by impairing SNAP29-mediated autophagosome-lysosome fusion. Cell Death & Disease. 2021; 12: 854. https://doi.org/10.1038/s41419-021-04138-0.

[12] Henrich MT, Oertel WH, Surmeier DJ, Geibl FF. Mitochondrial dysfunction in Parkinson's disease - a key disease hallmark with therapeutic potential. Molecular Neurodegeneration. 2023; 18: 83. https://doi.org/10.1186/s13024-023-00676-7.

[13] Pei F, Ma L, Jing J, Feng J, Yuan Y, Guo T, *et al*. Sensory nerve niche regulates mesenchymal stem cell homeostasis via FGF/mTOR/autophagy axis. Nature Communications. 2023; 14: 344. https://doi.org/10.1038/s41467-023-35977-4.

[14] Tu HY, Yuan BS, Hou XO, Zhang XJ, Pei CS, Ma YT, *et al*. $\alpha$-synuclein suppresses microglial autophagy and promotes neurodegeneration in a mouse model of Parkinson's disease. Aging Cell. 2021; 20: e13522. https://doi.org/10.1111/acel.13522.

[15] Zhang X, Wei M, Fan J, Yan W, Zha X, Song H, *et al*. Ischemia-induced upregulation of autophagy preludes dysfunctional lysosomal storage and associated synaptic impairments in neurons. Autophagy. 2021; 17: 1519–1542. https://doi.org/10.1080/15548627.2020.1840796.

[16] Wang H, Liu Y, Wang D, Xu Y, Dong R, Yang Y, *et al*. The Upstream Pathway of mTOR-Mediated Autophagy in Liver Diseases. Cells. 2019; 8: 1597. https://doi.org/10.3390/cells8121597.

[17] Cayo A, Segovia R, Venturini W, Moore-Carrasco R, Valenzuela C, Brown N. mTOR Activity and Autophagy in Senescent Cells, a Complex Partnership. International Journal of Molecular Sciences. 2021; 22: 8149. https://doi.org/10.3390/ijms22158149.

[18] Mustapha M, Mat Taib CN. MPTP-induced mouse model of Parkinson's disease: A promising direction of therapeutic strategies. Bosnian Journal of Basic Medical Sciences. 2021; 21: 422–433. https://doi.org/10.17305/bjbms.2020.5181.

[19] Huang P, Zhang Z, Zhang P, Feng J, Xie J, Zheng Y, *et al*. TREM2 Deficiency Aggravates NLRP3 Inflammasome Activation and Pyroptosis in MPTP-Induced Parkinson's Disease Mice and LPS-Induced BV2 Cells. Molecular Neurobiology. 2024; 61: 2590–2605. https://doi.org/10.1007/s12035-023-03713-0.

[20] Jang JS, Hong SJ, Mo S, Kim MK, Kim YG, Lee Y, *et al*. PINK1 restrains periodontitis-induced bone loss by preventing osteoclast mitophagy impairment. Redox Biology. 2024; 69: 103023. https://doi.org/10.1016/j.redox.2023.103023.

[21] Douiev L, Miller C, Ruppo S, Benyamini H, Abu-Libdeh B, Saada A. Upregulation of COX4-2 via HIF-1$\alpha$ in Mitochondrial COX4-1 Deficiency. Cells. 2021; 10: 452. https://doi.org/10.3390/cells10020452.

[22] Chen Z, Li G, Liu J. Autonomic dysfunction in Parkinson's disease: Implications for pathophysiology, diagnosis, and treatment. Neurobiology of Disease. 2020; 134: 104700. https://doi.org/10.1016/j.nbd.2019.104700.

[23] Gao C, Liu J, Tan Y, Chen S. Freezing of gait in Parkinson's disease: pathophysiology, risk factors and treatments. Translational Neurodegeneration. 2020; 9: 12. https://doi.org/10.1186/s40035-020-00191-5.

[24] Kamath T, Abdulraouf A, Burris SJ, Langlieb J, Gazestani V, Nadaf NM, *et al*. Single-cell genomic profiling of human dopamine neurons identifies a population that selectively degenerates in Parkinson's disease. Nature Neuroscience. 2022; 25: 588–595. https://doi.org/10.1038/s41593-022-01061-1.

[25] Zhang C, Zhao M, Wang B, Su Z, Guo B, Qin L, *et al*. The Nrf2-NLRP3-caspase-1 axis mediates the neuroprotective effects of Celastrol in Parkinson's disease. Redox Biology. 2021; 47: 102134. https://doi.org/10.1016/j.redox.2021.102134.

[26] Guo M, Liu W, Luo H, Shao Q, Li Y, Gu Y, *et al*. Hypoxic stress accelerates the propagation of pathological alpha-synuclein and degeneration of dopaminergic neurons. CNS Neuroscience & Therapeutics. 2023; 29: 544–558. https://doi.org/10.1111/cns.14055.

[27] Lin Z, Huang L, Cao Q, Luo H, Yao W, Zhang JC. Inhibition of abnormal C/EBP$\beta$/$\alpha$-Syn signaling pathway through activation of Nrf2 ameliorates Parkinson's disease-like pathology. Aging Cell. 2023; 22: e13958. https://doi.org/10.1111/acel.13958.

[28] Liu T, Wang P, Yin H, Wang X, Lv J, Yuan J, *et al*. Rapamycin reverses ferroptosis by increasing autophagy in MPTP/MPP$^+$-induced models of Parkinson's disease. Neural Regeneration Research. 2023; 18: 2514–2519. https://doi.org/10.4103/1673-5374.371381.

[29] Marogianni C, Sokratous M, Dardiotis E, Hadjigeorgiou GM, Bogdanos D, Xiromerisiou G. Neurodegeneration and Inflammation-An Interesting Interplay in Parkinson's Disease. International Journal of Molecular Sciences. 2020; 21: 8421. https://doi.org/10.3390/ijms21228421.

[30] Park H, Kam TI, Peng H, Chou SC, Mehrabani-Tabari AA, Song JJ, *et al*. PAAN/MIF nuclease inhibition prevents neurodegeneration in Parkinson's disease. Cell. 2022; 185: 1943–1959.e21. https://doi.org/10.1016/j.cell.2022.04.020.

[31] Zhang K, Zhu S, Li J, Jiang T, Feng L, Pei J, *et al*. Targeting autophagy using small-molecule compounds to improve potential therapy of Parkinson's disease. Acta Pharmaceutica Sinica. B. 2021; 11: 3015–3034. https://doi.org/10.1016/j.apsb.2021.02.016.

[32] Sorice M. Crosstalk of Autophagy and Apoptosis. Cells. 2022; 11: 1479. https://doi.org/10.3390/cells11091479.

[33] Li R, Lu Y, Zhang Q, Liu W, Yang R, Jiao J, *et al*. Piperine promotes autophagy flux by P2RX4 activation in *SNCA*/$\alpha$-synuclein-induced Parkinson disease model. Autophagy. 2022; 18: 559–575. https://doi.org/10.1080/15548627.2021.1937897.

[34] Zhong X, Wang B, Zhang G, Yuan Y, Hu X, Xiong J, *et al*. Autophagy Activation Is Involved in Acidic Fibroblast Growth Factor Ameliorating Parkinson's Disease *via* Regulating Tribbles Homologue 3. Frontiers in Pharmacology. 2019; 10: 1428. https://doi.org/10.3389/fphar.2019.01428.

[35] Nechushtai L, Frenkel D, Pinkas-Kramarski R. Autophagy in Parkinson's Disease. Biomolecules. 2023; 13: 1435. https://doi.org/10.3390/biom13101435.

[36] Singh F, Prescott AR, Rosewell P, Ball G, Reith AD, Ganley IG. Pharmacological rescue of impaired mitophagy in Parkinson's disease-related LRRK2 G2019S knock-in mice. eLife. 2021; 10: e67604. https://doi.org/10.7554/eLife.67604.

[37] Geng X, Zou Y, Li S, Qi R, Yu H, Li J. MALAT1 Mediates $\alpha$-Synuclein Expression through miR-23b-3p to Induce Autophagic Impairment and the Inflammatory Response in Microglia to Promote Apoptosis in Dopaminergic Neuronal Cells. Mediators of Inflammation. 2023; 2023: 4477492. https://doi.org/10.1155/2023/4477492.

[38] Zhang Z, Sun X, Wang K, Yu Y, Zhang L, Zhang K, *et al*. Hydrogen-saturated saline mediated neuroprotection through autophagy via PI3K/AKT/mTOR pathway in early and medium stages of rotenone-induced Parkinson's disease rats. Brain Research Bulletin. 2021; 172: 1–13. https://doi.org/10.1016/j.brainresbull.2021.04.003.

[39] Son SM, Siddiqi FH, Lopez A, Ansari R, Tyrkalska SD, Park SJ, *et al*. Alpha-synuclein mutations mislocalize cytoplasmic p300 compromising autophagy, which is rescued by ACLY inhibition. Neuron. 2025; 113: 1908–1924.e13. https://doi.org/10.1016/j.neuron.2025.03.028.

[40] Pan Y, Chen M, Pan L, Tong Q, Cheng Z, Lin S, *et al*. Shisandra Decoction Alleviates Parkinson's Disease Symptoms in a Mouse Model Through PI3K/AKT/mTOR Signalling Pathway. Neuropsychiatric Disease and Treatment. 2024; 20: 2011–2027. https://doi.org/10.2147/NDT.S476969.

[41] Li Y, Yuan Y, Li Y, Han D, Liu T, Yang N, *et al*. Inhibition of $\alpha$-Synuclein Accumulation Improves Neuronal Apoptosis and Delayed Postoperative Cognitive Recovery in Aged Mice. Oxidative Medicine and Cellular Longevity. 2021; 2021: 5572899. https://doi.org/10.1155/2021/5572899.